


# Superconductivity in a misfit compound (PbSe)<sub>1.12</sub>(TaSe<sub>2</sub>)

Xiaohui Yang<sup>1,2</sup>, Mengmeng Wang<sup>1,2</sup>, Yupeng Li<sup>1,2</sup>, Hua Bai<sup>1,2</sup>, Jiang Ma<sup>1,2</sup>,  
Xikang Sun<sup>1,2</sup>, Qian Tao<sup>1,2</sup>, Cheng Dong<sup>3</sup> and Zhu-An Xu<sup>1,2,4</sup> 

<sup>1</sup> Zhejiang Province Key Laboratory of Quantum Technology and Device and Department of Physics, Zhejiang University, Hangzhou 310027, People's Republic of China

<sup>2</sup> State Key Laboratory of Silicon Materials, Zhejiang University, Hangzhou 310027, People's Republic of China

<sup>3</sup> Institute of Physics, Chinese Academy of Sciences, Beijing 100190, People's Republic of China

<sup>4</sup> Zhejiang California International NanoSystems Institute, Zhejiang University, Hangzhou 310058, People's Republic of China

E-mail: [zhuan@zju.edu.cn](mailto:zhuan@zju.edu.cn)

Received 7 September 2018, revised 29 September 2018

Accepted for publication 11 October 2018

Published 2 November 2018



## Abstract

We report the discovery of superconductivity with a maximum  $T_c \approx 1.28$  K in Br-doped (PbSe)<sub>1.12</sub>(TaSe<sub>2</sub>), which is a new misfit compound consisting of alternating layers of distorted rocksalt PbSe and dichalcogenide TaSe<sub>2</sub>. It is found that the Br-doping is required for the formation of this misfit compound and superconductivity can be tuned by the Br content. The large anisotropic parameter of resistivity  $\gamma_\rho = \rho_c / \rho_{ab} \approx 100$  and that of the upper critical field  $\gamma_{H_{c2}} = H_{c2}^{ab} / H_{c2}^c \approx 10$  are obtained. The estimated  $c$ -axis coherence length  $\xi_c \approx 6.3$  nm, larger than the  $c$ -axis lattice constant, which implies that this compound is an anisotropic three-dimensional superconductor. The Hall coefficient measurements suggest that the charge transport is dominated by the hole-type charge carrier and there is a charge transfer from the PbSe layer to the conducting TaSe<sub>2</sub> layer. The small normalized specific heat jump  $\Delta C / \gamma T_c = 1.16$  and electron–phonon coupling constant  $\lambda_{ep} \approx 0.61$  indicate that Br-doped (PbSe)<sub>1.12</sub>(TaSe<sub>2</sub>) is a weak coupling Bardeen–Cooper–Schrieffer superconductor.

**Keywords:** misfit chalcogenide, weak coupling BCS superconductor, charge carrier density, anisotropic superconductivity

(Some figures may appear in colour only in the online journal)

## 1. Introduction

The unique structures and properties of misfit layered chalcogenide compounds (MLCs) have attracted much attention recently [1–7]. They are described by the general formula  $(MX)_{1+\delta}(TX_2)_m$ , where  $M$  is Sn, Pb, Sb, Bi or a lanthanide;  $T$  is Ti, V, Nb, Ta or Cr;  $X$  is S, Se or Te;  $0.08 \leq \delta \leq 0.28$  and  $m = 1, 2, 3$  [8, 9]. The structure is generally regarded as an alternating sequence of dichalcogenide  $TX_2$  layers interleaved between the distorted rocksalt-type  $MX$  layers along the  $c$  direction. Because the two interleaved layers display different symmetry and periodicity, they match along the  $b$ -axis direction and a mismatch occurs in the  $a$ -axis direction, resulting in an incommensurate structure [10, 11]. The non-

integer  $1 + \delta$  indicates the degree of misfit, which can be determined by the ratio of in-plane packing density of each constituent [11, 12]. The most reported MLCs are synthesized by usual high temperature solid state reaction or the chemical vapor transport (CVT) method [4, 13, 14]. Recently the so-called ‘ferrecrystals’ with the same formula were produced by the physical vapor deposition method, these have much rotational disorder between the layers and thus display different properties [15, 16]. It is generally believed that the physical properties of MLCs are dominated by the dichalcogenide layers, which demonstrate rich ground states [12]. For example,  $1T$ -TiSe<sub>2</sub> and  $2H$ -TaSe<sub>2</sub> exhibit a charge density wave (CDW) phase transition near 200 K and 92 K, respectively [17, 18].  $2H$ -TaSe<sub>2</sub>,  $2H$ -TaS<sub>2</sub> and  $2H$ -NbSe<sub>2</sub> show

superconductivity at 0.15 K, 0.8 K and 7.2 K, respectively [19, 20]. The MLCs like  $(\text{LaSe})_{1.14}(\text{NbSe}_2)$  and  $(\text{SnS})_{1.15}(\text{TaSe}_2)$  containing superconducting  $\text{NbSe}_2$  and  $\text{TaSe}_2$  sublayers show superconductivity at 1.32 K and 3.01 K respectively [6, 21]. Moreover, due to the intercalation of rocksalt  $\text{MX}$  layers, the MLCs could exhibit drastically different physical properties compared to the native dichalcogenide  $\text{TX}_2$  layers. The misfit layered compound  $(\text{PbSe})_{1.16}(\text{TiSe}_2)_2$  containing  $\text{TiSe}_2$  sublayers has been widely studied over the last few years, and is reported to be a superconductor at  $T_c = 2.3$  K without CDW phase transition [4, 5, 22].

Because of diverse  $M$ ,  $X$ ,  $T$  and  $m$ , there are a large number of misfit layered compounds with vastly different physical properties [23]. Therefore, it is worthwhile to synthesize new MLCs and investigate their physical properties. Furthermore, the natural heterostructures can be built by the specially alternating layers with van der Waals forces, which provide an interesting potential opportunity to study the effect of interface structure and the influence of charge transfer between the adjacent layers [24]. In this work, we report the discovery of superconductivity in a new misfit compound Br-doped  $(\text{PbSe})_{1.12}(\text{TaSe}_2)$  with a maximum  $T_c \approx 1.28$  K. It is found that  $T_c$  as well as the carrier concentration monotonically decreases for low Br content. A strong anisotropy of this compound is observed in both the resistivity and upper critical field. The specific heat jump at  $T_c$  and the deduced electron–phonon coupling parameter suggest that this misfit compound  $(\text{PbSe})_{1.12}(\text{TaSe}_2)$  is a weak coupling Bardeen–Cooper–Schrieffer (BCS) superconductor.

## 2. Experimental

The single crystals of Br-doped  $(\text{PbSe})_{1.12}(\text{TaSe}_2)$  were prepared by the CVT method using  $\text{PbBr}_2$  as the transport agent. Since Br atom can occupy on the Se sites both in the  $\text{PbSe}$  layer and the  $\text{TaSe}_2$  layer, thus a simplified chemical formula  $\text{Pb}_{1.12}\text{TaSe}_{3.12}$  instead of  $(\text{PbSe})_{1.12}(\text{TaSe}_2)$  is used for the Br-doped case. The high-purity Pb, Ta, Se and  $\text{PbBr}_2$  powders were thoroughly mixed in the appropriate ratios with nominal composition  $\text{Pb}_{1.12}\text{Ta}(\text{Se}_{1-x}\text{Br}_x)_{3.12}$  ( $x = 0.05, 0.1, 0.15, 0.2$ ) in Ar gas atmosphere. The resulting powders were sealed in evacuated silica tubes with a diameter of 12 mm and length of 18 cm, and then heated for a week in a two-zone furnace, where the temperatures of source zone and cold zone were fixed at 900 °C and 800 °C respectively. Large single crystals were obtained in the middle of the tube with a typical dimension of  $5 \times 5 \times 0.2$  mm.

The single crystal x-ray diffraction (XRD) and powder XRD were carried out at room temperature using a PANalytical x-ray diffractometer (Model EMPYREAN) with a monochromatic  $\text{Cu-K}_{\alpha 1}$  radiation. The composition of the materials were determined by an x-ray energy dispersive spectrometer (EDS) affiliated to a Hitachi S-3700N scanning electronic microscope. High-resolution transmission electron microscopy (HRTEM) and the selected area electron diffraction (SAED) images were

obtained by an aberration corrected FEI-Titan G2 80-200 ChemiSTEM operated at 100 kV. The temperature dependence of electrical resistivity were measured on an Oxford superconducting magnet system equipped with a  $^3\text{He}$  cryostat. The heat capacity measurements were performed in a Quantum Design physical property measurement system employing a relaxation method.

## 3. Results and discussion

Figures 1(a) and (d) show the schematics of the misfit crystal structure of  $(\text{PbSe})_{1.12}(\text{TaSe}_2)$  along different directions. It composed of alternating rocksalt-type  $\text{PbSe}$  layers and  $\text{TaSe}_2$  layers along the  $c$ -axis. Figures 1(b) and (e) display the corresponding HRTEM images of Br-doped  $(\text{PbSe})_{1.12}(\text{TaSe}_2)$  taken along the  $[100]$  and  $[010]$  direction respectively, indicating the regular stacking of bi-layer  $\text{PbSe}$  and three atom thick  $\text{TaSe}_2$  blocks. The resulting SAED patterns are shown in figures 1(c) and (f). Figure 1(c) shows a typical SAED pattern with electron beam along  $[100]$ , the reflections show the staking periodicity of 23.47 Å along the  $c$ -axis direction and 5.92 Å along the  $b$ -axis direction, this observation confirms that the  $\text{TaSe}_2$  and  $\text{PbSe}$  subsystems match along the  $b$ -axis direction. Figure 1(f) shows an SAED pattern taken along the commensurate  $b$ -axis direction, containing two sets of reflections of the  $\text{TaSe}_2$  and  $\text{PbSe}$  subsystems, which are indicated by the arrows in different colors. From this zone axis SAED, the periodicity of 23.47 Å along the  $c$ -axis direction, 6.097 Å for  $\text{PbSe}$  and 3.41 Å for  $\text{TaSe}_2$  along the  $a$ -axis direction were identified. The mismatch factor  $\delta$  can be defined by the formula  $1 + \delta = 2 * a_2/a_1$ , where  $a_1$  and  $a_2$  are the  $a$ -axis lattice parameters of  $\text{MX}$  and  $\text{TX}_2$  sublayers [25]. We then obtain the incommensurate factor  $1 + \delta \approx 1.12$ , which agrees well with the average value of 1.09 determined by chemical analysis.

The powder XRD pattern of  $\text{Pb}_{1.12}\text{Ta}(\text{Se}_{0.92}\text{Br}_{0.08})_{3.12}$  crushed single crystals is shown in figure 2(a). Because the single crystals are too malleable to grind into fine powders, we added a small amount of Si powder to help on grinding the single crystals thoroughly before gathering XRD data. The powder pattern with a high level of preferred orientation can be well indexed by the  $\text{PbSe}$  and  $\text{TaSe}_2$  subsystems, and the obtained lattice parameters are given in table 1. The lattice constants are consistent with the reported data in the literature [26, 27]. The chemical compositions were also measured by EDS, and the Br content in the single crystals  $\text{Pb}_{1.12}\text{Ta}(\text{Se}_{1-x}\text{Br}_x)_{3.12}$  are determined to be  $x = 0.08, 0.10, 0.14, 0.16$  respectively. As a representative, an EDS pattern with electron beams focused on the selected area of  $\text{Pb}_{1.12}\text{Ta}(\text{Se}_{0.92}\text{Br}_{0.08})_{3.12}$  single crystal are shown in the inset of figure 2(a). The single crystal XRD patterns of a series of  $\text{Pb}_{1.12}\text{Ta}(\text{Se}_{1-x}\text{Br}_x)_{3.12}$  single crystals are displayed in figure 2(b). Only multiple reflections of  $(00l)$  peaks can be observed, indicating a uniform  $c$ -axis orientation perpendicular to the plane of the single crystals. In the inset of figure 2(b), the full width at half maximum of the  $(0016)$  peaks is only  $0.05^\circ$ , demonstrating the good quality of the samples,

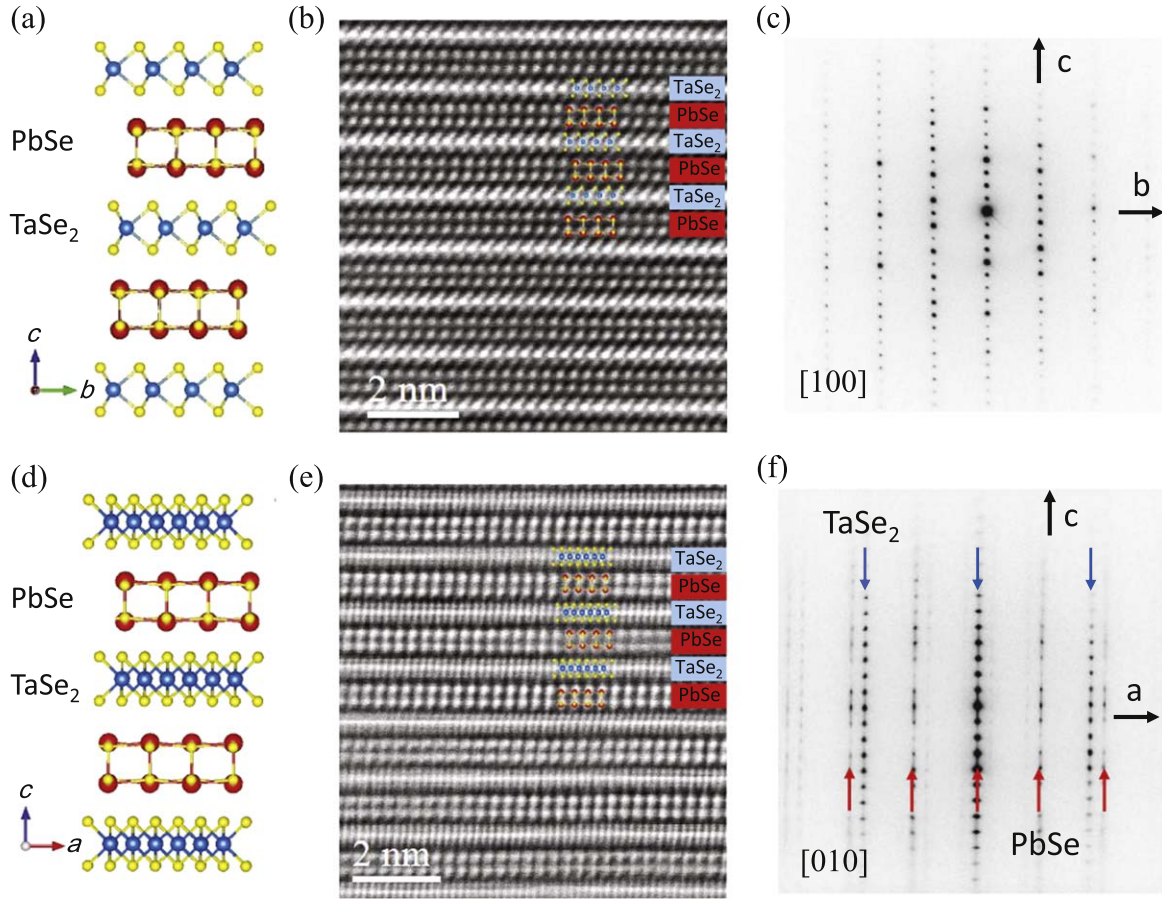


**Figure 1.** The crystal structure of  $(\text{PbSe})_{1.12}(\text{TaSe}_2)$ . (a) Along the  $a$ -direction. (d) Along the  $b$ -direction. HRTEM images and corresponding SAED patterns of  $\text{Pb}_{1.12}\text{Ta}(\text{Se}_{0.92}\text{Br}_{0.08})_{3.12}$ , (b) and (c) taken along the  $[100]$  zone axis, (e) and (f) taken along the  $[010]$  zone axis. Blue arrow:  $\text{TaSe}_2$  subsystem; red arrow:  $\text{PbSe}$  subsystem.

and the  $(0016)$  peak shifts systematically towards the higher angle region with increasing Br concentration. The lattice parameter  $c$  as a function of actual Br content  $x$  was presented in figure 2(c). The  $c$ -axis lattice parameter shows a significant shrink with increasing Br content, which is consistent with the smaller ion radius of Br compared to Se. Overall, it is confirmed that all samples were Br-doped and the doping content was limited up to  $x = 0.18$  due to the solubility limit.

Figure 3(a) shows the temperature dependence of the electrical resistivity for the  $\text{Pb}_{1.12}\text{Ta}(\text{Se}_{1-x}\text{Br}_x)_{3.12}$  single crystals. An expanded plot of the low temperature regime below 1.5 K is presented in the inset, and sharp superconducting transitions are clearly observed. Using the 50% normal-state resistivity criterion, the maximum  $T_c$  of about 1.28 K is reached at  $x = 0.08$ .  $T_c$  firstly decreases with increasing Br content and finally increases for  $x > 0.14$ . The origin of anomalous increase in  $T_c$  for larger Br content needs further investigation. The temperature dependence of in-plane resistivity  $\rho_{ab}$  and out-plane resistivity  $\rho_c$  for the optimal sample  $\text{Pb}_{1.12}\text{Ta}(\text{Se}_{0.92}\text{Br}_{0.08})_{3.12}$  are presented in figure 3(c). They both exhibit metallic behavior and superconducting transitions at low temperatures. A large anisotropic ratio  $\gamma_p = \rho_c/\rho_{ab} \approx 100$  is obtained over the whole temperature range, which is much larger than that of non-superconducting  $(\text{PbSe})_{1.12}(\text{TiSe}_2)$  ( $\gamma_p \sim 20$ ) and that of  $(\text{LaSe})_{1.14}\text{NbSe}_2$

superconductor ( $\gamma_p \sim 50$ ) [5, 28], but comparable to that of  $(\text{SnSe})_{1.16}\text{NbSe}_2$  superconductor ( $\gamma_p \sim 100$ ) [7]. The large anisotropy should be attributed to the highly anisotropic structure.

Figures 4(a) and (b) show the temperature dependence of resistivity  $\rho_{ab}$  under a magnetic field applied perpendicularly and parallel to the  $ab$ -plane respectively. The superconducting transition shifts toward lower temperatures with increasing magnetic fields, indicating a field-induced pair breaking effect. Taking the criterion of 50% of the normal-state value, the resulted  $H_{c2}$  is summarized in figure 4(c) with the theoretical fits using the Werthamer–Helfand–Hohenberg formula [29]. The estimated  $H_{c2}^{ab}(0) = 1.15$  T and  $H_{c2}^c(0) = 0.15$  T. Obviously,  $H_{c2}(0)$  in both direction is lower than the Pauli limit field, i.e.,  $\mu_0 H_p^{\text{BCS}}(0) = 1.84 T_c \sim 2.4$  T. The anisotropy of upper critical field,  $\gamma_{H_{c2}} = H_{c2}^{ab}/H_{c2}^c$ , is about 10 near  $T_c$ . The zero temperature Ginzburg–Landau coherence length is estimated by  $H_{c2}^c = \Phi_0/2\pi\xi_{ab}^2$  and  $H_{c2}^{ab} = \Phi_0/2\pi\xi_{ab}\xi_c$  for both directions, and  $\xi_{ab}(0) \approx 42.8$  nm and  $\xi_c(0) \approx 6.3$  nm are obtained. Apparently,  $\xi_c(0)$  is larger than the distance of two successive superconducting layers and the anisotropy factor  $\gamma_{H_{c2}}$  decreases slightly down to 0.3 K, demonstrating that the misfit compound behaves as a three-dimensional anisotropic superconductor.

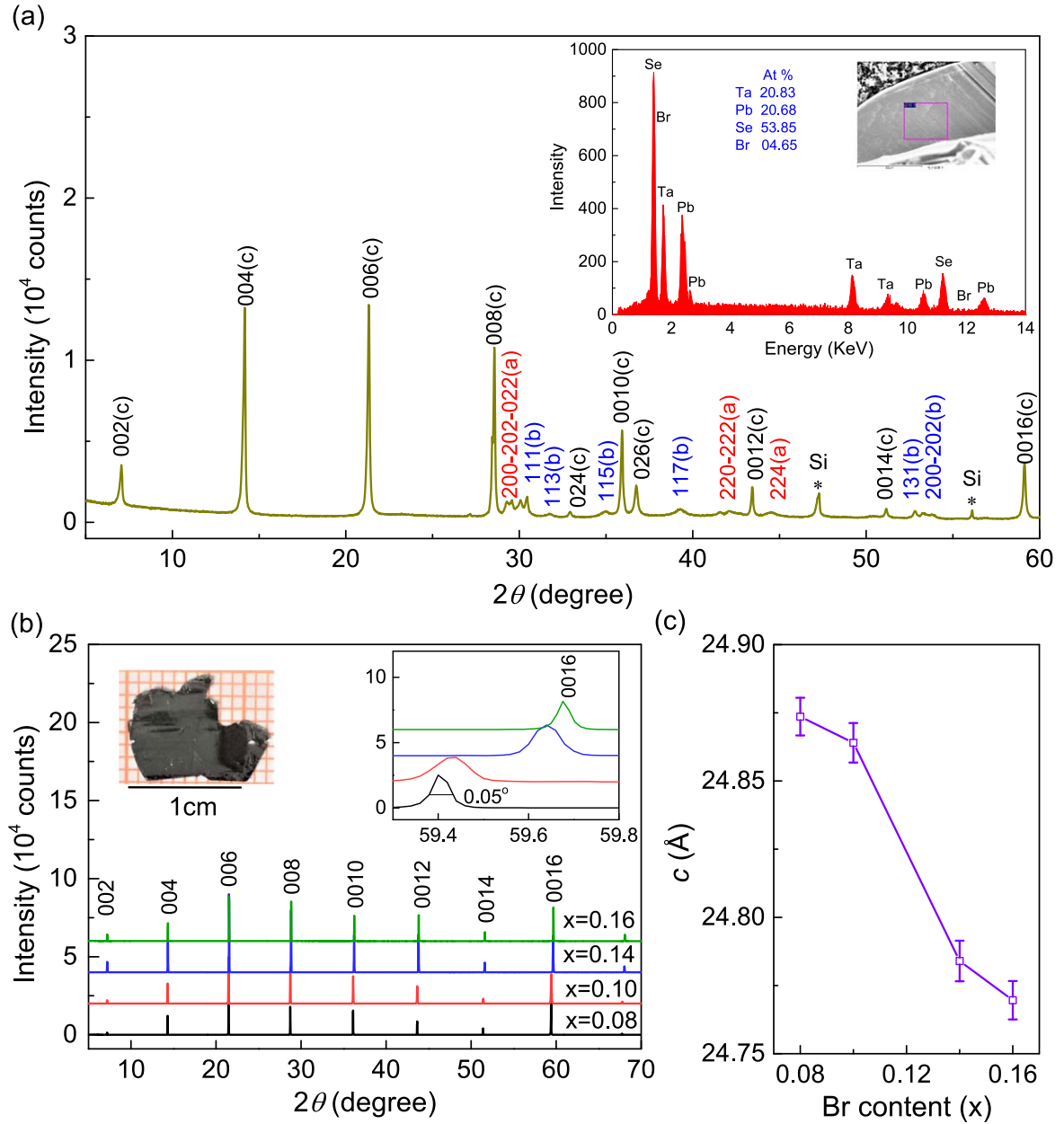


**Figure 2.** (a) Powder XRD pattern of  $\text{Pb}_{1.12}\text{Ta}(\text{Se}_{0.92}\text{Br}_{0.08})_{3.12}$  compound. ‘a’ represents the  $\text{PbSe}$  subsystem, ‘b’ represents the  $\text{TaSe}_2$  subsystem, ‘c’ represents the common reflections with indices of the  $\text{TaSe}_2$  subsystem. Peaks from Si are marked by asterisks. Inset: a typical energy dispersive x-ray spectrum of  $\text{Pb}_{1.12}\text{Ta}(\text{Se}_{0.92}\text{Br}_{0.08})_{3.12}$  single crystal, the obtained atom ratios were also displayed. (b) Single crystal x-ray diffraction patterns of  $\text{Pb}_{1.12}\text{Ta}(\text{Se}_{1-x}\text{Br}_x)_{3.12}$  single crystals. The different patterns are offset vertically for clarity. Left inset is the photograph of  $\text{Pb}_{1.12}\text{Ta}(\text{Se}_{0.92}\text{Br}_{0.08})_{3.12}$  single crystal, right inset displays the shifting of the (0016) peak. (c) Lattice parameter  $c$  as a function of Br content  $x$ .

**Table 1.** The lattice parameters of  $\text{Pb}_{1.12}\text{Ta}(\text{Se}_{0.92}\text{Br}_{0.08})_{3.12}$ .

Subsystem	$a$ (Å)	$b$ (Å)	$c$ (Å)	Space group
$\text{PbSe}$	6.160	6.105	25.049	Fm2m
$\text{TaSe}_2$	3.435	6.027	25.034	Fm2m

Figure 5(a) shows the Hall coefficient ( $R_H$ ) as a function of temperature of  $\text{Pb}_{1.12}\text{Ta}(\text{Se}_{1-x}\text{Br}_x)_{3.12}$  single crystals. The positive  $R_H$  steadily decreases upon increasing the temperature below 100 K and becomes almost constant in the high

temperature range, indicating that the hole-type carriers are dominant. Since the Hall resistivity is linearly dependent on magnetic fields, we use a single-band model to estimate carrier concentration  $n_H = 1/eR_H$ .  $n_H$  at 1.5 K and  $T_c$  determined at 50% normal-state resistivity with respect to Br content are presented in figure 5(b). It can be found that  $n_H$  monotonically decreases with increasing Br concentration and  $T_c$  decreases substantially by the initial Br substitution and reaches a minimum around  $x = 0.14$ , implying a close correlation between  $n_H$  and  $T_c$ . The change in charge carrier concentration can be interpreted by a charge transfer model



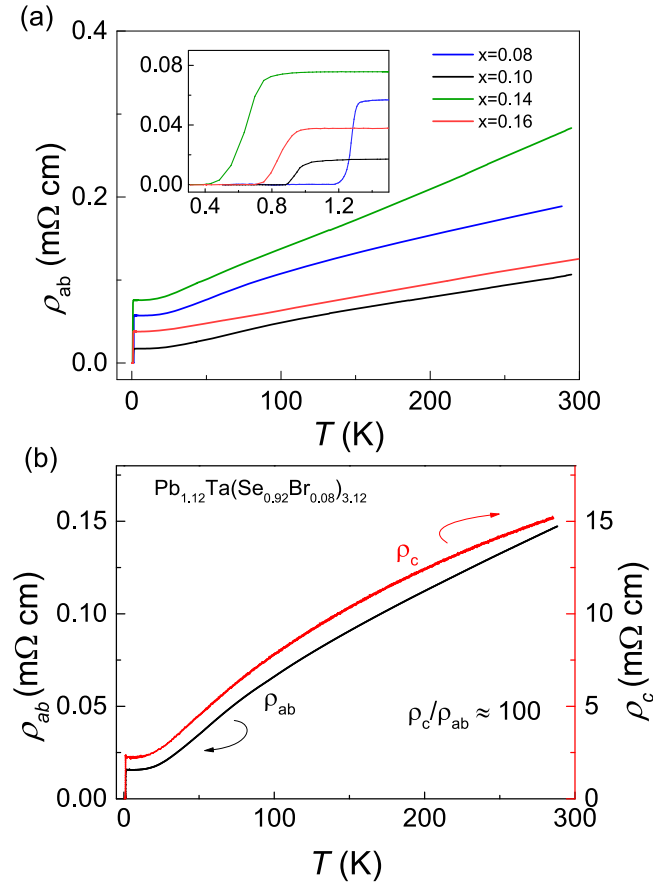


**Figure 3.** (a) Temperature dependence of the electrical resistivity  $\rho_{ab}$  for  $\text{Pb}_{1.12}\text{Ta}(\text{Se}_{1-x}\text{Br}_x)_{3.12}$  single crystals. The inset shows the superconducting transition below 1.5 K. (b) Temperature dependence of  $\rho_{ab}$  and  $\rho_c$  for  $\text{Pb}_{1.12}\text{Ta}(\text{Se}_{0.92}\text{Br}_{0.08})_{3.12}$  single crystal.

shown in the inset, a schematic of a general proposal for PbSe and TaSe<sub>2</sub> electronic states near the Fermi level in  $(\text{PbSe})_{1.12}(\text{TaSe}_2)$ . Such a charge transfer model was proposed for the misfit compound  $(\text{PbSe})_{1.14}(\text{NbSe}_2)$  [30], and these two compounds should have almost the same electronic structure [31]. In the rigid band-like model, the overlap of the Se 4p states in the PbSe layer with the Ta- $d_{z^2}$  states can be clearly found. Thus spontaneous potential charge transfer occurs from the PbSe layer to the TaSe<sub>2</sub> layer due to the different chemical potentials, resulting in the presence of holes in the PbSe layer. A similar scenario is also proposed in the misfit compound  $(\text{PbSe})_{1.16}(\text{TiSe}_2)_2$ , and the electron transfer from PbSe layers to TiSe<sub>2</sub> layers has recently been confirmed by a study of angle-resolved photoemission spectroscopy [4, 24]. The decrease in hole-type carrier concentration caused by Br-doping is in agreement with the additional electron doping induced by Br substituting on the Se site.

Figure 6 plots the specific heat divided by temperature  $C_p/T$ , as a function of  $T^2$  of the  $\text{Pb}_{1.12}\text{Ta}(\text{Se}_{0.92}\text{Br}_{0.08})_{3.12}$  single crystal. The normal-state specific heat at low temperature obeys the relation of  $C_p/T = \gamma + \beta T^2$ , where  $\gamma$  and  $\beta$  are the coefficient of electronic specific heat and phonon specific heat. The linear fit yields the  $\gamma = 6.34 \text{ mJ mol}^{-1} \text{ K}^{-2}$  and  $\beta = 5.82 \text{ mJ mol}^{-1} \text{ K}^{-4}$ . The Debye temperature  $\Theta_D = 119 \text{ K}$  is

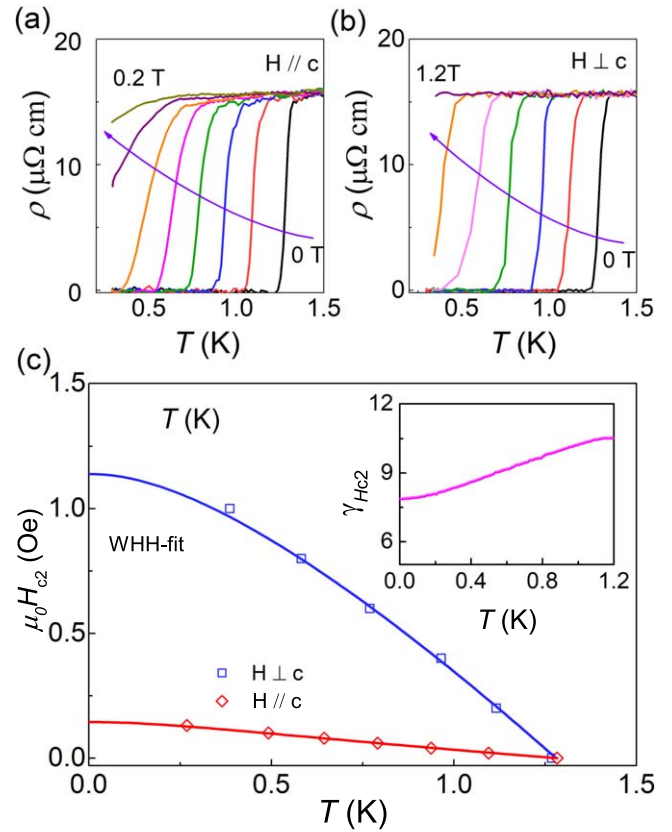


**Figure 4.** The low temperature resistivity under different magnetic fields of  $\text{Pb}_{1.12}\text{Ta}(\text{Se}_{0.92}\text{Br}_{0.08})_{3.12}$ . (a) Magnetic field perpendicular to the  $ab$ -plane. (b) Magnetic field parallel to the  $ab$ -plane. (c) Temperature dependence of the upper critical field  $H_{c2}$  of  $\text{Pb}_{1.12}\text{Ta}(\text{Se}_{0.92}\text{Br}_{0.08})_{3.12}$ . Inset: temperature dependence of the anisotropy factor  $\gamma_{Hc2}$ .

estimated by the relation  $\beta = (12\pi^4 n R) / 5 \Theta_D^3$ , where  $n$  is the number of atoms per formula unit ( $n = 5$ ) without considering mismatch index  $\delta$  and  $R$  is the gas constant.  $C_e$  was obtained by subtracting the phonon contribution from measured specific data. The normalized electronic specific heat  $C_e/\gamma T$  as a function of reduced temperature  $T/T_c$  is shown in the inset. By fitting the one gap BCS  $\alpha$ -model:  $C_e = C_0 \exp(-\Delta/k_B T)$  ( $\alpha = \Delta/k_B T_c$ ), the obtained  $\alpha = 1.64$  is comparable to the value  $\alpha_{\text{BCS}} = 1.76$  of weakly coupled BCS superconductors [32]. We estimated the normalized specific heat jump  $\Delta C/\gamma T_c = 1.16$ , which is smaller than the BCS weak coupling limit (1.43), but close to the values in other misfit compounds such as  $(\text{SnSe})_{1.14}(\text{TiSe}_2)(0.88)$  and  $(\text{SnS})_{1.15}(\text{TaS}_2)(0.81)$  [6, 25]. The electron-phonon coupling constant  $\lambda_{e-ph} \approx 0.61$  is estimated from the McMillan formula by assuming  $\mu^* = 0.15$  for the Coulomb pseudo-potential [33]

$$\lambda_{ep} = \frac{1.04 + \mu^* \ln\left(\frac{\Theta_D}{1.45 T_c}\right)}{(1 - 0.62 \mu^*) \ln\left(\frac{\Theta_D}{1.45 T_c}\right) - 1.04}.$$

The  $\lambda_{ep}$  value suggests this compound is a weak coupling superconductor. With the value  $\lambda_{ep}$  and  $\gamma$ , the density of states at

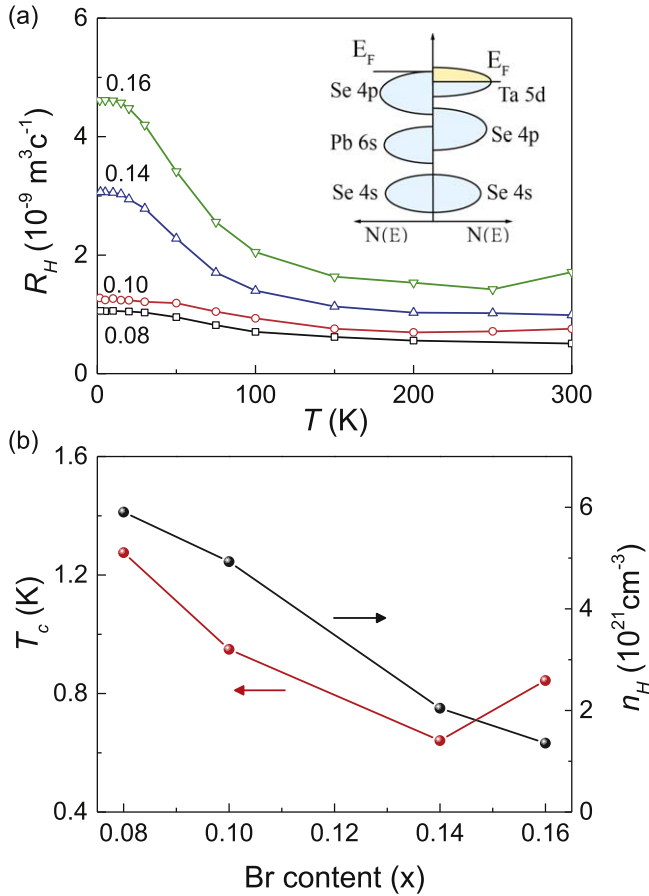


**Figure 5.** (a) Temperature dependence of the Hall coefficient for  $\text{Pb}_{1.12}\text{Ta}(\text{Se}_{1-x}\text{Br}_x)_{3.12}$  single crystals. Inset: a proposed schematic electronic band structure of  $(\text{PbSe})_{1.12}(\text{TaSe}_2)$ . (b)  $T_c$  and carrier concentration  $n_H$  as a function of the doping content  $x$ .

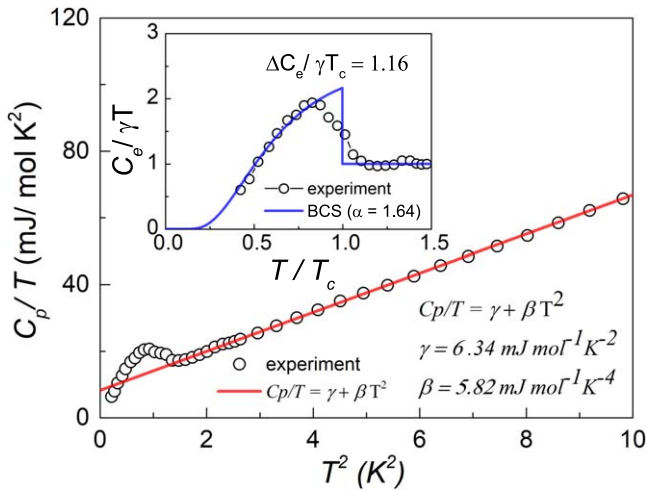


**Figure 6.** The temperature dependence of the specific heat  $C_p$  of  $\text{Pb}_{1.12}\text{Ta}(\text{Se}_{0.92}\text{Br}_{0.08})_{3.12}$ , presented in the form of  $C_p/T$  versus  $T^2$ . Inset: reduced temperature  $T/T_c$  dependence of normalized electronic specific heat  $C_e/\gamma T$ .

Fermi level  $[N(E_F)]$  can be calculated using the equation  $N(E_F) = \frac{3}{\pi^2(k_B)^2(1 + \lambda_{ep})}\gamma$ . The estimated value  $N(E_F) = 1.67$  states/eV f.u for  $\text{Pb}_{1.12}\text{Ta}(\text{Se}_{0.92}\text{Br}_{0.08})_{3.12}$ , which is close to that of the transition metal dichalcogenide  $2\text{H-TaSe}_2$  [34].

## 4. Conclusion

In summary, we have successfully grown the single crystals of misfit compounds  $\text{Pb}_{1.12}\text{Ta}(\text{Se}_{1-x}\text{Br}_x)_{3.12}$  ( $0.08 \leq x \leq 0.16$ ) with a maximum  $T_c \approx 1.28$  K. Superconductivity is gradually suppressed by the initial Br substitution ( $x < 0.14$ ) and then enhanced slightly with further doping. Distinct anisotropy of resistivity and upper critical field of  $\text{Pb}_{1.12}\text{Ta}(\text{Se}_{0.92}\text{Br}_{0.08})_{3.12}$  single crystal was detected. The out-of-plane coherence length  $\xi_c$  is larger than the distance between the superconducting ( $\text{TaSe}_2$ ) layers, indicating that this compound behaves as a 3D anisotropic superconductor. The Hall effect measurements confirm that Br-doping is an electron type dopant, and the decrease in hole carrier concentration could destroy superconductivity. In addition, the electronic heat capacity of  $\text{Pb}_{1.12}\text{Ta}(\text{Se}_{0.92}\text{Br}_{0.08})_{3.12}$  demonstrates that the misfit compound is a weak coupling superconductor.

## Acknowledgments

The authors would like to thank Xin Lu, Zhen Wang and Xiaojun Yang for helpful discussions. This work was supported by the National Key R&D Projects of China (grant no. 2016YFA0300402), the National Science Foundation of China (grant no. 11774305), and the Fundamental Research Funds for the Central Universities of China.

## ORCID iDs

Zhu-An Xu <https://orcid.org/0000-0001-9290-2762>

## References

- [1] Wieggers G A, Meetsma A, Haange R J and De Boer J L 1988 *Mater. Res. Bull.* **23** 1551
- [2] Cava R J, Batlogg B, van Dover R B, Ramirez A P, Krajewski J J, Peck W F and Rupp L W 1994 *Phys. Rev. B* **49** 6343
- [3] Ren Y, Rüscher C H, Haas C and Wieggers G A 2002 *J. Phys.: Condens. Matter* **14** 8011
- [4] Giang N, Xu Q, Hor Y S, Williams A J, Dutton S E, Zandbergen H W and Cava R J 2010 *Phys. Rev. B* **82** 024503
- [5] Wang N Z, Yuan S F, Cong R, Lu X F, Meng F B, Shang C and Chen X H 2015 *Europhys. Lett.* **112** 67007
- [6] Sankar R, Peramaiyan G, Muthuselvan I P, Wen C Y, Xu X F and Chou F C 2018 *Chem. Mater.* **30** 1373
- [7] Bai H et al 2018 *J. Phys.: Condens. Matter* **30** 355701
- [8] Wieggers G A, Meetsma A, Haange R J and De Boer J L 1990 *J. Solid State Chem.* **89** 328
- [9] Wieggers G A and Meerschaut A 1992 *J. Alloys Compd.* **178** 351
- [10] Wieggers G A 1995 *J. Alloys Compd.* **219** 152
- [11] Ren Y, Baas J, Meetsma A, De Boer J L and Wieggers G A 1996 *Acta Crystallogr. B* **52** 398
- [12] Merrill D R, Moore D B, Bauers S R, Falmbigl M and Johnson D C 2015 *Materials* **8** 2000

- [13] Wiegers G A, Meetsma A, Haange R J and de Boer J L 1992 *J. Alloys Compd.* **178** 369
- [14] Oosawa Y, Gotoh Y, Akimoto J, Tsunoda T, Sohma M and Onoda M 1992 *Japan. J. Appl. Phys.* **31** L1096
- [15] Moore D B, Beekman M, Disch S, Zschack P, Häusler I, Neumann W and Johnson D C 2013 *Chem. Mater.* **25** 2404
- [16] Wood S R, Merrill D R, Falmbigl M, Moore D B, Ditto J, Esters M and Johnson D C 2015 *Chem. Mater.* **27** 6067
- [17] Di Salvo F J, Moncton D E and Waszczak J V 1976 *Phys. Rev. B* **14** 4321
- [18] Naito M and Tanaka S 1982 *J. Phys. Soc. Japan.* **51** 219
- [19] Yokota K, Kurata G, Matsui T and Fukuyama H 2000 *Physica B* **284** 551
- [20] Wilson J A, Di Salvo F J and Mahajan S 1975 *Adv. Phys.* **24** 117
- [21] Nader A, Lafond A, Briggs A, Meerschaut A and Roesky R 1998 *Synth. Met.* **97** 147
- [22] Luo H X, Yan K, Pletikoscic I, Xie W W, Phelan B F, Valla T and Cava R J 2016 *J. Phys. Soc. Japan.* **85** 064705
- [23] Wiegers G A 1996 *Prog. Solid State Chem.* **24** 1
- [24] Yao Q *et al* 2018 *Phys. Rev. Lett.* **120** 106401
- [25] Song Y J, Kim M J, Jung W G, Kim B J and Rhyee J S 2016 *Phys. Status Solidi B* **253** 1517
- [26] Auriel C, Roesky R, Meerschaut A and Rouxel J 1993 *Mater. Res. Bull.* **28** 247
- [27] Zhou W Y, Meetsma A, de Boer J L and Wiegers G A 1992 *Mater. Res. Bull.* **27** 563
- [28] Szabó P, Samuely P, Kačmarčík J, Jansen A G M, Briggs A, Lafond A and Meerschaut A 2001 *Phys. Rev. Lett.* **86** 5990
- [29] Werthamer N R, Helfand E and Hohenberg P C 1966 *Phys. Rev.* **147** 295
- [30] Alemayehu M B, Mitchson G, Ditto J, Hanken B E, Asta M and Johnson D C 2014 *Chem. Mater.* **26** 1859
- [31] Rouxel J, Meerschaut A and Wiegers G A 1995 *J. Alloys Compd.* **229** 144
- [32] Padamsee H, Neighbor J E and Shiffman C A 1973 *J. Low Temp. Phys.* **12** 387
- [33] McMillan W L 1968 *Phys. Rev.* **167** 331
- [34] Bhoi D, Khim S, Nam W, Lee B S, Kim C, Jeon B G, Min B H, Park S and Kim K H 2016 *Sci. Rep.* **6** 24068